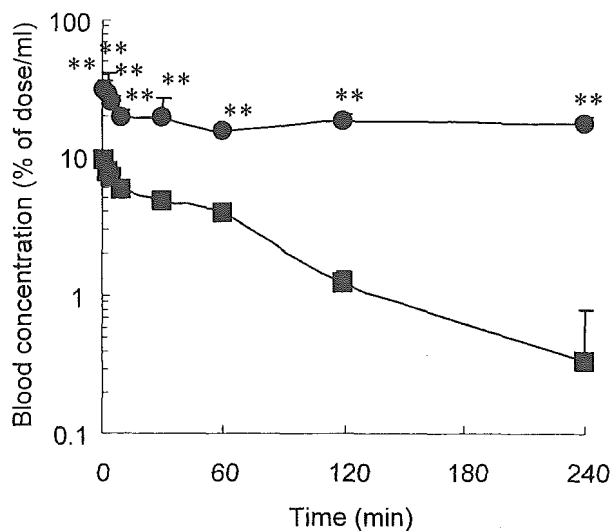


**Figure 1.** Blood concentration of [<sup>3</sup>H] ATRA (■) and [<sup>3</sup>H] ATRA (●) or [<sup>3</sup>H] CHE (○) incorporated in liposomes following intravenous administration in mice. Each value represents the mean + SD of three experiments. Statistically significant differences from [<sup>3</sup>H] ATRA (\*\**p* < 0.01; [<sup>3</sup>H] ATRA in liposomes, ##*p* < 0.01; [<sup>3</sup>H] CHE in liposomes).

In order to achieve the incorporation of lipophilic drugs, a high number of benzyl groups were introduced into the poly(aspartic acid) chain. Thus, ATRA is expected to be stably incorporated in the hydrophobic inner core of the polymeric micelles. Figure 2 shows the blood concentration profiles of [<sup>3</sup>H] ATRA dispersed in serum (inherent distribution of ATRA) and [<sup>3</sup>H] ATRA incorporated in polymeric micelles (Bz-75) after intravenous injection until 240 min. The blood concentration of [<sup>3</sup>H] ATRA in mouse serum was significantly lower than that of [<sup>3</sup>H] ATRA in polymeric micelles (Bz-75), suggesting that polymeric micelles with benzyl groups can enhance the blood retention by their encapsulation.

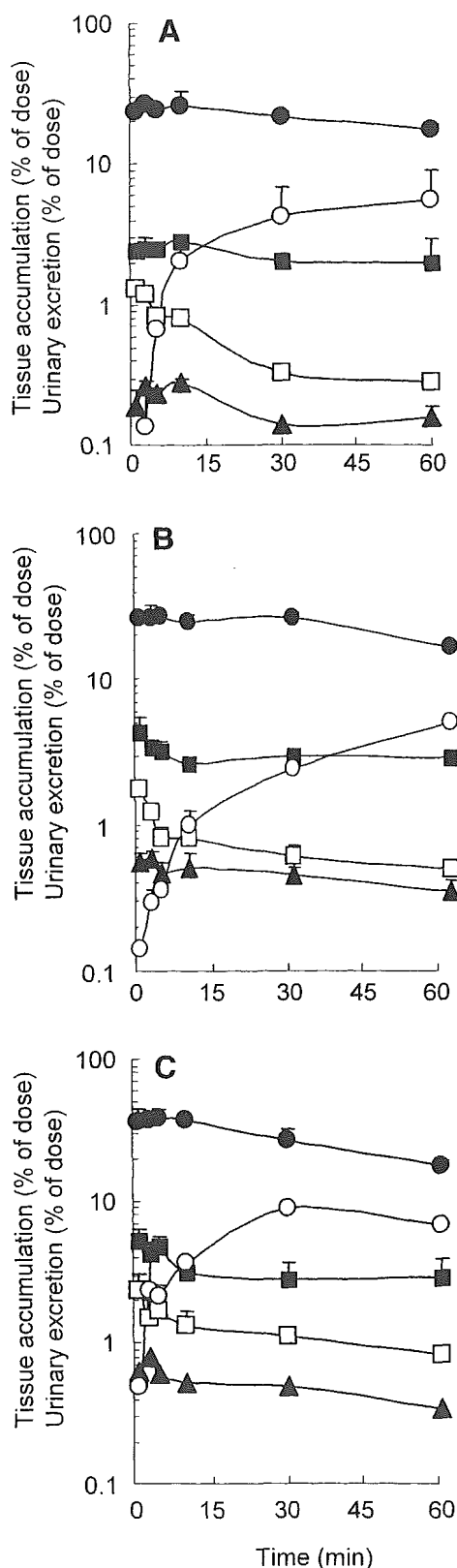
#### Tissue Distribution and Pharmacokinetic Analyses of [<sup>3</sup>H]ATRA, [<sup>3</sup>H]ATRA Incorporated in Liposomes or Polymeric Micelles

Figure 3 shows the tissue distribution profiles of [<sup>3</sup>H]ATRA (A), [<sup>3</sup>H]ATRA incorporated in liposomes (B), or polymeric micelles (Bz-75) (C). Regardless of the formulation, most of the ATRA was recovered from the liver, kidney, and urine.



**Figure 2.** Blood concentration of [<sup>3</sup>H] ATRA (■) and [<sup>3</sup>H] ATRA (●) incorporated in polymeric micelles (Bz-75) following intravenous administration in mice. Each value represents the mean + SD of three experiments. Statistically significant differences from [<sup>3</sup>H] ATRA (\*\**p* < 0.01).

In order to clarify the distribution characteristics of ATRA, ATRA incorporated in liposomes or polymeric micelles, a pharmacokinetic analysis was performed. Analyzing the disposition profiles of ATRA incorporated in polymeric micelles, the initial distribution during the early phase up to 10 min, in which the contribution of metabolism can be ignored, was quantified using organ clearance parameters. Table 1 summarizes the area under the blood concentration-time profile ( $AUC_{\text{blood}}$ ) and the uptake clearance for ATRA, ATRA incorporated in liposomes, and polymeric micelles (Bz-75). The  $AUC_{\text{blood}}$  of ATRA incorporated in polymeric micelles (Bz-75) and liposomes was 2.8- and 1.2-times higher than ATRA, indicating the enhanced the blood retention of ATRA. The uptake clearances were determined for liver ( $CL_{\text{liver}}$ ), kidney ( $CL_{\text{kidney}}$ ), spleen ( $CL_{\text{spleen}}$ ), lung ( $CL_{\text{lung}}$ ), and heart ( $CL_{\text{heart}}$ ) and the hepatic uptake clearances were the highest among the tissues examined for both groups suggesting that the liver is the main organ for ATRA uptake. In addition, the  $CL_{\text{liver}}$  of ATRA incorporated in polymeric micelles (Bz-75) and liposomes was lower than ATRA; therefore, this lower liver uptake could reflect the higher  $AUC_{\text{blood}}$  of ATRA incorporated in polymeric micelles (Bz-75) and liposomes.



### *In Vitro* Release of ATRA from ATRA in Polymeric Micelles

Figure 4 shows the *in vitro* penetration of ATRA from ATRA in polymeric micelles through dialysis membrane. The penetration of ATRA from ATRA in polymeric micelles to receiver side was very low until 20 h. In the presence of 20% DMSO in donor and receiver side, however, the penetration of ATRA from ATRA in polymeric micelles was much enhanced.

### DISCUSSION

The purpose of this study was to examine the biodistribution characteristics of ATRA incorporated in liposomes and polymeric micelles (Bz-75) after intravenous administration. Our findings indicate that both carriers influence the biodistribution of ATRA although the incorporation efficacy is different.

In preclinical and clinical trials, it has been reported that ATRA incorporated in liposomes can maintain a higher ATRA concentration in plasma than oral administration of ATRA.<sup>5,6</sup> In this case, however, the administration route is different; therefore the effect of liposomes on ATRA distribution after intravenous administration remains unclear. To clarify the effect of the carrier system, the inherent distribution of ATRA must be examined. Because the water solubility of ATRA is too low ( $<0.1 \mu\text{g/mL}$  at  $20^\circ\text{C}$ ), solubilizing agents must be used for intravenous administration. Some organic solvents, for example, propylene glycol or ethanol are sometimes used, but this has the disadvantage the precipitation can occur following dilution of blood. In order to avoid such a problem, mouse serum was selected as a dissolving agent to analyze the inherent distribution of ATRA after intravenous administration.

Liposomes are widely used as carriers for a variety of drugs including ATRA. However, the distribution profiles of liposomes depending on the lipid composition; in particular, the cholesterol content of the liposomes is an important factor

**Figure 3.** Tissue accumulation and urinary excretion of [ $^3\text{H}$ ] ATRA (A), [ $^3\text{H}$ ] ATRA incorporated in liposomes (B), and polymeric micelles (Bz-75) (C) following intravenous administration in mice. Each value represents the mean + SD of three experiments. Radioactivity was determined in the liver (●), urine (○), kidney (■), spleen (▲), and lung (□).

**Table 1.** Area Under Blood Concentration-Time Curve ( $AUC_{\text{blood}}$ ) and Tissue Uptake and Urinary Excretion Clearance for ATRA, ATRA in Liposomes, and Polymeric Micelles (Bz-75) after Intravenous Administration

Sample	$AUC_{\text{blood}}$ (% of dose · h/mL) <sup>a</sup>	Tissue uptake clearance <sup>a</sup> ( $\mu\text{L}/\text{h}$ )				
		$CL_{\text{liver}}$	$CL_{\text{kidney}}$	$CL_{\text{spleen}}$	$CL_{\text{lung}}$	$CL_{\text{urine}}$
ATRA	1.59	16318	1783	173	507	1277
ATRA in liposomes	1.92	12887	1393	266	423	522
ATRA in polymeric micelle	4.43	8307	706	177	295	823

<sup>a</sup> $AUC_{\text{blood}}$  and tissue uptake clearance were calculated for the initial phase of the experiment until 10 min after intravenous administration.

*in vivo*.<sup>25,26</sup> We previously reported that DSPC/Chol (6:4) liposomes were more stable than DSPC/Chol (9:1) and DSPC/Chol (7:3) liposomes in blood.<sup>27</sup> Therefore, DSPC/Chol (6:4) liposomes were selected as a carrier of ATRA in this study because the purpose of this study was to achieve enhanced blood retention of ATRA *in vivo*. We have shown that the blood concentration of ATRA was more sustained when ATRA were incorporated in DSPC/Chol (6:4) liposomes (Fig. 1), indicating that liposomes can control the distribution of ATRA for sustained blood retention to some extent. This result reflects the effectiveness of liposomal ATRA in clinical situations with regard to APL therapy after intravenous administration.

In the systemic circulation, drugs incorporated into liposomes are diluted by the blood, followed by interaction with plasma components; consequently, incorporated drugs are rapidly released from liposomes.<sup>18,27-29</sup> Even if liposomes exhibit a favorable *in vivo* disposition profile, rapid release

of incorporated drugs would lead to a failure to achieve therapeutic potency. Therefore, the inherent distribution profiles of liposomes were also examined using [<sup>3</sup>H] CHE in order to confirm the contribution of controlled ATRA distribution by the liposomes. We have shown that the blood concentration of [<sup>3</sup>H] ATRA incorporated in liposomes was much lower than that of [<sup>3</sup>H] CHE incorporated in liposomes (Fig. 1), suggesting that most ATRA are rapidly released from liposomes in the blood. These results indicate that in order to achieve further blood retention of ATRA by the carrier system, ATRA release must be controlled *in vivo*.

Among the various particulate carrier systems available to date, polymeric micelles are an effective drug carrier. In this study, we tried to apply polymeric micelles to ATRA delivery *in vivo* for sustained blood retention. Polymeric micelles have a small particle size and are expected to avoid RES trapping while the protective effect offered by the hydrophilic outer shell could reduce the interaction between the carrier and biological components. After intravenous injection of ATRA incorporated in polymeric micelles (Bz-75), blood concentration of ATRA was significantly higher than that of ATRA dispersed in serum (inherent distribution of ATRA) (Fig. 2). In addition, pharmacokinetic analysis demonstrated that ATRA incorporated in the polymeric micelles (Bz-75) exhibits a larger  $AUC_{\text{blood}}$  and lower hepatic clearance of ATRA when compared with ATRA and ATRA incorporated in liposomes (Tab. 1). These results suggested that ATRA incorporated in polymeric micelles (Bz-75) reduces RES scavenging.

ATRA was almost completely incorporated in polymeric micelles (Bz-75) (>95%) and ATRA release from ATRA incorporated in polymeric micelles (Bz-75) was very low until 20 h (Fig. 4). These results suggested that ATRA was very stably incorporated in polymeric micelles (Bz-75).

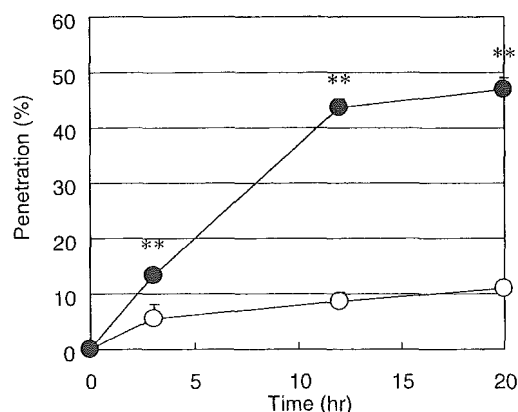


**Figure 4.** In vitro release of ATRA from ATRA incorporated in polymeric micelles (Bz-75) in phosphate buffered saline (O) or 20% DMSO phosphate buffered saline (●). Each value represents the mean + SD of three experiments. Statistically significant differences from phosphate buffered saline (\*\* $p < 0.01$ ).

In order to confirm whether ATRA release was enhanced by hydrophobic components, the release experiments in the presence of 20% DMSO phosphate buffered saline was performed. As shown in Figure 4, ATRA release was much enhanced in the presence of 20% DMSO, suggesting that ATRA release was enhanced by hydrophobic components in the body. However, these results also indicated that ATRA release was still controlled even in the presence of 20% DMSO. This result is in accordance with *in vivo* finding that ATRA concentration was sustained following the intravenous injection of ATRA incorporated in polymeric micelles (Fig. 2).

Recently, ATRA is also used as a chemopreventive agent, which exerts strong antitumor activity by suppressing tumor growth.<sup>31–34</sup> However, like many other anticancer drugs, sophisticated targeting is required for successful *in vivo* application. It has been reported that polymeric micelles in the size range <200 nm reduce nonselective RES scavenging and exhibit enhanced permeability and retention effects (EPR)<sup>35</sup> at solid tumor sites for passive targeting. Although further study is required, ATRA incorporated in polymeric micelles (Bz-75) could be useful for cancer differentiation therapy employing the EPR effect in the future.

Jeong et al.<sup>30</sup> developed a poly( $\epsilon$ -caprolactone)/poly(ethylene glycol) diblock copolymer for ATRA incorporation. They examined the ATRA incorporation and ATRA release into polymeric micelles and demonstrated that ATRA incorporation efficacy is increased by the molecular weight of hydrophobic poly( $\epsilon$ -caprolactone) in the poly( $\epsilon$ -caprolactone)/poly(ethylene glycol) diblock copolymer. Their observation about the incorporation of ATRA *in vitro* agrees with our *in vivo* results. Since ATRA is a highly lipophilic drug ( $\log PC_{oct} = 6.6$ );<sup>16</sup> more lipophilic conditions in the inner core of the polymeric micelles might be required for stable ATRA incorporation.

In conclusion, we have examined the biodistribution characteristics of ATRA incorporated in liposomes and polymeric micelles following intravenous administration. Among them, we have shown that polymeric micelles (Bz-75) are the most effective carrier of ATRA for sustained blood retention *in vivo*. Furthermore, it appears that ATRA release under *in vivo* conditions is governed by the physicochemical properties of the hydrophobic chain in the block copolymer. These results have potential implications for the design of ATRA carriers for APL patients.

## ACKNOWLEDGMENTS

This work was supported in part by Grants-in-Aid for Scientific Research from the Ministry of Education, Culture, Sports, Science, and Technology of Japan, and by Health and Labor Sciences Research Grants for Research on Hepatitis and BSE from the Ministry of Health, Labor and Welfare of Japan (No. 15–21). The authors thank Sachiko Suzuki, Tomoyuki Okuda, Yuuki Kamiya, and Chittima Managit for technical assistance.

## REFERENCES

- Huang ME, Ye YC, Chen SR, Chai J, Lu JX, Zhou L, Gu LJ, Wang ZY. 1998. Use of all-trans retinoic acid in the treatment of acute promyelocytic leukemia. *Blood* 72:567–572.
- Castaigne S, Chomienne C, Daniel MT, Ballerini P, Berger R, Fenoux P, Degos L. 1990. All-trans retinoic acid as a differentiation therapy for acute promyelocytic leukemia. I. Clin results *Blood* 76:1704–1709.
- Muindi J, Frankel SR, Miller WH, Jr, Jakubowski A, Scheinberg DA, Young CW, Dmitrovsky E, Warrell RP, Jr. 1992. Continuous treatment with all-trans retinoic acid causes a progressive reduction in plasma drug concentrations: Implications for relapse and retinoid “resistance” in patients with acute promyelocytic leukemia. *Blood* 79:299–303.
- Mehta K, Sadeghi T, McQueen T, Lopez-Berestein G. 1994. Liposome encapsulation circumvents the hepatic clearance mechanisms of all-trans-retinoic acid. *Leuk Res* 18:587–596.
- Ozpolat B, Lopez-Berestein G, Adamson P, Fu CJ, Williams AH. 2003. Pharmacokinetics of intravenously administered liposomal all-trans-retinoic acid (ATRA) and orally administered ATRA in healthy volunteers. *J Pharm Sci* 6:292–301.
- Estey E, Thall PF, Mehta K, Rosenblum M, Brewer T, Jr, Simmons V, Cabanillas F, Kurzrock R, Lopez-Berestein G. 1996. Alterations in tretinoin pharmacokinetics following administration of liposomal all-trans retinoic acid. *Blood* 87:3650–3654.
- Estey EH, Giles FJ, Kantarjian H, O'Brien S, Cortes J, Freireich EJ, Lopez-Berestein G, Keating M. 1999. Molecular remissions induced by liposomal-encapsulated all-trans retinoic acid in newly diagnosed acute promyelocytic leukemia. *Blood* 94:2230–2235.
- Douer D, Estey E, Santillana S, Bennett JM, Lopez-Berestein G, Boehm K, Williams T. 2001. Treatment of newly diagnosed and relapsed acute promyelocytic leukemia with intravenous liposomal all-trans retinoic acid. *Blood* 97:73–80.

9. Lim SJ, Kim CK. 2002. Formulation parameters determining the physicochemical characteristics of solid lipid nanoparticles loaded with all-trans retinoic acid. *Int J Pharm* 243:135–146.
10. Hwang SR, Lim SJ, Park JS, Kim CK. 2004. Phospholipid-based microemulsion formulation of all-trans-retinoic acid for parenteral administration. *Int J Pharm* 276:175–183.
11. Yokoyama M, Miyauchi M, Yamada N, Okano T, Sakurai Y, Kataoka K, Inoue S. 1990. Characterization and anticancer activity of the micelle-forming polymeric anticancer drug adriamycin-conjugated poly(ethylene glycol)-poly(aspartic acid) block copolymer. *Cancer Res* 50:1693–1700.
12. Yokoyama M, Satoh A, Sakurai Y, Okano T, Matsumura Y, Kakizoe T, Kataoka K. 1998. Incorporation of water-insoluble anticancer drug into polymeric micelles and control of their particle size. *J Control Release* 55:219–229.
13. Nishiyama N, Yokoyama M, Aoyagi T, Okano T, Sakurai Y, Kataoka K. 1999. Preparation and characterization of self-assembled polymer-metal complex micelle from *cis*-dichlorodiammineplatinum (II) and poly(ethyleneglycol)-poly( $\alpha$ ,  $\beta$ -aspartic acid) block copolymer in an aqueous medium. *Langmuir* 15:377–383.
14. Yokoyama M, Kwon GS, Okano T, Sakurai Y, Seto T, Kataoka K. 1992. Preparation of micelle-forming polymer-drug conjugates. *Bioconjug Chem* 3:295–301.
15. Opanasopit P, Yokoyama M, Watanabe M, Kawano K, Maitani Y, Okano T. 2004. Block copolymer design for camptothecin incorporation into polymeric micelles for passive tumor targeting. *Pharm Res* 21:2001–2008.
16. Takino T, Nakajima C, Takakura Y, Sezaki H, Hashida M. 1993. Controlled biodistribution of highly lipophilic drugs with various parenteral formulations. *J Drug Target* 1:117–124.
17. Kawakami S, Ohshima N, Hirayama R, Hirai M, Kitahara T, Sakaeda T, Mukai T, Nishida K, Nakamura J, Nakashima M, Sasaki H. 2002. Biodistribution and pharmacokinetics of *O*-palmitoyl tilisolol, a lipophilic prodrug of tilisolol, after intravenous administration in rats. *Biol Pharm Bull* 25:1072–1076.
18. Hattori Y, Kawakami S, Yamashita F, Hashida M. 2000. Controlled biodistribution of galactosylated liposomes and incorporated probucol in hepatocyte-selective drug targeting. *J Control Release* 69:369–377.
19. Kawakami S, Munakata C, Fumoto S, Yamashita F, Hashida M. 2000. Targeted delivery of prostaglandin  $E_1$  to hepatocytes using galactosylated liposomes. *J Drug Target* 8:137–142.
20. Kawakami S, Wong J, Sato A, Hattori Y, Yamashita F, Hashida M. 2000. Biodistribution characteristics of mannosylated, fucosylated, and galactosylated liposomes in mice. *Biochim Biophys Acta* 1524:258–265.
21. Yokoyama M, Opanasopit P, Okano T, Kawano K, Maitani Y. 2004. Polymer design and incorporation methods for polymeric micelle carrier system containing water-insoluble anti-cancer agent camptothecin. *J Drug Target* 12:373–384.
22. Kawakami S, Yamamura K, Mukai T, Nishida K, Nakamura J, Sakaeda T, Nakashima M, Sasaki H. 2001. Sustained ocular delivery of tilisolol to rabbits after topical administration or intravitreal injection of lipophilic prodrug incorporated in liposomes. *J Pharm Pharmacol* 53:1157–1161.
23. Takakura Y, Takagi A, Hashida M, Sezaki H. 1987. Disposition and tumor localization of mitomycin C-dextran conjugates in mice. *Pharm Res* 4:293–300.
24. Kawakami S, Munakata C, Fumoto S, Yamashita F, Hashida M. 2001. Novel galactosylated liposomes for hepatocyte-selective targeting of lipophilic drugs. *J Pharm Sci* 90:105–113.
25. Murao A, Nishikawa M, Managit C, Wong J, Kawakami S, Yamashita F, Hashida M. 2002. Targeting efficiency of galactosylated liposomes to hepatocytes in vivo: Effect of lipid composition. *Pharm Res* 19:1808–1814.
26. Kirby C, Clarke J, Gregoriadis G. 1980. Effect of the cholesterol content of small unilamellar liposomes on their stability in vivo and in vitro. *Biochem J* 186:591–598.
27. Senior J, Gregoriadis G. 1982. Stability of small unilamellar liposomes in serum and clearance from the circulation: The effect of the phospholipid and cholesterol components. *Life Sci* 30:2123–2136.
28. Harashima H, Sakata K, Funato K, Kiwada H. 1994. Enhanced hepatic uptake of liposomes through complement activation depending on the size of liposomes. *Pharm Res* 11:402–406.
29. Teshima M, Kawakami S, Nishida K, Nakamura J, Sakaeda T, Terazono H, Kitahara T, Nakashima M, Sasaki H. 2004. Prednisolone retention in integrated liposomes by chemical approach and pharmaceutical approach. *J Control Release* 97:211–218.
30. Jeong YI, Kang MK, Sun HS, Kang SS, Kim HW, Moon KS, Lee KJ, Kim SH, Jung S. 2004. All-trans-retinoic acid release from core-shell type nanoparticles of poly(epsilon-caprolactone)/poly(ethylene glycol) diblock copolymer. *Int J Pharm* 273:95–107.
31. Falasca L, Favale A, Gualandi G, Maietta G, Conti Devirgiliis L. 1998. Retinoic acid treatment induces apoptosis or expression of a more differentiated phenotype on different fractions of cultured fetal rat hepatocytes. *Hepatology* 28:727–737.
32. Ohlmann CH, Jung C, Jaques G. 2002. Is growth inhibition and induction of apoptosis in lung cancer cell lines by fenretinide [*N*-(4-hydroxyphenyl)retinamide] sufficient for cancer therapy? *Int J Cancer* 100:520–526.

33. Choi Y, Kim SY, Kim SH, Yang J, Park K, Byun Y. 2003. Inhibition of tumor growth by biodegradable microspheres containing all-trans-retinoic acid in a human head-and-neck cancer xenograft. *Int J Cancer* 107:145–148.
34. Shimizu K, Tamagawa K, Takahashi N, Takayama K, Maitani Y. 2003. Stability and antitumor effects of all-trans retinoic acid-loaded liposomes contained sterylglucoside mixture. *Int J Pharm* 258:45–53.
35. Matsumura Y, Maeda H. 1986. A new concept for macromolecular therapeutics in cancer chemotherapy: Mechanism of tumorotropic accumulation of proteins and the antitumor agent smancs. *Cancer Res* 46:6387–6392.

# Enhanced gene expression in lung by a stabilized lipoplex using sodium chloride for complex formation

Shigeru Kawakami  
Yoshitaka Ito  
Shintaro Fumoto  
Fumiyoshi Yamashita  
Mitsuru Hashida\*

Department of Drug Delivery  
Research, Graduate School of  
Pharmaceutical Sciences, Kyoto  
University, Sakyo-ku, Kyoto  
606-8501, Japan

\*Correspondence to:  
Mitsuru Hashida, Department of  
Drug Delivery Research, Graduate  
School of Pharmaceutical Sciences,  
Kyoto University, Sakyo-ku, Kyoto  
606-8501, Japan. E-mail:  
hashidam@pharm.kyoto-u.ac.jp

## Abstract

**Background** In this study, we investigated the *in vivo* gene transfection efficacy of a 'surface charge regulated' (SCR) lipoplex, dispersed in the presence of an essential amount of NaCl during lipoplex formation.

**Methods** SCR lipoplexes were prepared and their physicochemical properties were analyzed. After intravenous (i.v.) administration, transfection efficacy, distribution characteristics, and liver toxicity were evaluated in mice.

**Results** At NaCl concentrations of 10 mM, the particle sizes of the SCR lipoplexes were about 120 nm and were compatible with a conventional lipoplex. However, fluorescent resonance energy transfer analysis revealed that cationic liposomes in the SCR lipoplexes increased fusion. After i.v. administration, the transfection activity in the lung of the SCR lipoplex (10 mM NaCl solution in the lipoplex) was approximately 10-fold higher than that of the conventional lipoplex. Pharmacokinetic studies demonstrated a higher distribution in lung by the SCR lipoplex. When the gene expression levels of the SCR lipoplex and conventional lipoplex were compared, the SCR lipoplex at a dose of 30 µg was compatible with that of the conventional lipoplex at a dose of 50 µg. A significantly higher serum alanine aminotransferase (ALT) activity and TNF $\alpha$  concentration was observed by the conventional lipoplex (pDNA dose; 50 µg), but this was not the case for the SCR lipoplex (pDNA dose; 30 µg).

**Conclusions** We demonstrated that the SCR lipoplex could enhance the transfection efficacy in the lung without increasing the liver toxicity. Hence, the information will be valuable for the future use, design, and development of lipoplexes for *in vivo* applications. Copyright © 2005 John Wiley & Sons, Ltd.

**Keywords** gene therapy; cationic liposomes; non-viral vectors; lipoplex; toxicity

## Introduction

The ability to introduce gene-encoding therapeutic proteins into various tissues by systemic administration represents an important advance in gene therapy. Therefore, increasing attention has focused on the development of efficient non-viral vectors. The use of non-viral vectors has attracted great interest for *in vivo* gene delivery because they are free from some of the risks inherent in these other systems. Furthermore, the characteristics of non-viral vectors can be more easily modified than those of viral

Received: 16 March 2005  
Revised: 12 May 2005  
Accepted: 2 June 2005

vectors. In particular, much effort has been devoted to the development of cationic liposome-mediated gene delivery systems due to their favorable characteristics. Recently, several studies have shown that intravenous administration of plasmid DNA (pDNA)–cationic liposome complexes (i.e. lipoplexes) leads to systemic gene expression, particularly in the lung [1–5].

To date, several methods involving the systemic administration of lipoplex have been tested in order to enhance the transfection efficacy in the lung. Several parameters have been identified as important for achieving a high level of gene expression. These include the charge ratio between the cationic lipid and pDNA and the dose of pDNA [4,6,7]. Despite the enhanced transfection efficacy due to the excess cationic charge of the lipoplex or excess dose of pDNA, their clinical applications are hampered by their toxicity, including lethal effects in experimental animals [6,7]. Therefore, transfection efficacy needs to be enhanced by another approach before clinical application is possible, and simple methodologies are required to achieve this aim.

Lipoplexes are often prepared in a non-ionic solution due to their well-known tendency to aggregate out of solution as the salt concentration is increased [8,9]. Aggregation during lipoplex formation in ionic solution may be due to neutralization of the surface positive charge of the lipoplex intermediate by the associated counter ion. Taking account of neutralization by a counter ion, we hypothesized that the presence of an essential amount of sodium chloride (NaCl) during lipoplex formation might control the repulsion between cationic liposomes and the fusion of cationic liposomes in the lipoplex would be accelerated by partial neutralization of the positive charge. Consequently, pDNA in the lipoplex could be largely covered by cationic lipids while retaining enough positive charge to prevent aggregate formation. Such types of lipoplex are expected to be more stable than the conventional lipoplex, which is prepared using a non-ionic solution.

In a previous study, we investigated the *in vivo* gene transfection efficacy of a galactosylated 'surface charge regulated' (SCR) lipoplex, prepared in the presence of an essential amount of NaCl during lipoplex formation for hepatocyte-selective transfection [10]. We have already demonstrated that the galactosylated SCR lipoplex significantly delayed aggregation and the hepatic transfection activity of the galactosylated SCR lipoplex was approximately 10–20-fold higher than that of the conventional galactosylated lipoplex in mice. Thus, the SCR method is expected to be a novel approach for the stabilization of lipoplexes in the body.

Since intravenous (i.v.) administration of lipoplex induces the highest gene expression in the lung, we expected that the SCR lipoplex would enhance the gene expression in the lung due to the stabilizing effects based on the delayed aggregation. In the present study, we investigated the physicochemical properties and *in vivo* gene transfection characteristics of the SCR lipoplex after i.v. administration. Results were compared with those of

the conventional lipoplex, which was prepared using 5% dextrose as a solvent.

## Materials and methods

### Materials

*N*-[1-(2,3-Dioleoyloxy)propyl]-*N,N,N*-trimethylammonium chloride (DOTMA) was obtained from Tokyo Chemical Industry Co. (Tokyo, Japan). Cholesterol (Chol) was obtained from Nacalai Tesque Inc. (Kyoto, Japan). 1,2-Dioleoyl-*sn*-glycero-3-phosphoethanolamine-*N*-(7-nitro-2-1,3-benzoxadiazol-4-yl) (NBD-DOPE) and 1,2-dioleoyl-*sn*-glycero-3-phosphoethanolamine-*N*-(lissamine rhodamine B sulfonyl) (Rh-DOPE) were purchased from Avanti Polar Lipids, Inc. (AL, USA). [ $\alpha$ - $^{32}$ P]-dCTP (3000 Ci/mmol) was obtained from Amersham Co. (Tokyo, Japan). All other chemicals were of the highest purity available.

### Construction and preparation of pDNA

pcMV-Luc was constructed by subcloning the Hind III/Xba I firefly luciferase cDNA fragment from the pGL3-control vector (Promega Co., Madison, WI, USA) into the polylinker of the pcDNA3 vector (Invitrogen, Carlsbad, CA, USA). pDNA was amplified in the *E. coli* strain DH5 $\alpha$ , isolated, and purified using a Qiagen Endofree Plasmid Giga kit (Qiagen GmbH, Hilden, Germany). Finally, pDNA solution was dissolved in 5% dextrose solution and subjected to ultrafiltration using a Viaspin 2 (5000 MWCO; Vivascience AG, Hannover, Germany) to remove the salts. Purity was confirmed by 1% agarose gel electrophoresis followed by ethidium bromide staining and the pDNA concentration was measured by UV absorption at 260 nm. The pDNA for distribution experiments was labeled with [ $\alpha$ - $^{32}$ P]-dCTP by nick translation [11].

### Preparation of cationic liposomes

DOTMA/Chol liposomes were prepared as reported previously [5,8,12–14]. Mixtures of DOTMA and Chol were dissolved in chloroform at a molar ratio of 1:1, vacuum-desiccated, and resuspended in sterile 5% dextrose at a concentration of 4 mg total lipids per ml. The suspension was sonicated for 3 min and the resulting liposomes were extruded 10 times through 100 nm polycarbonate membrane filters.

### Preparation of conventional and SCR lipoplexes

Conventional and SCR lipoplexes were prepared as reported previously [10]. For conventional lipoplex



preparation, a volume of 600  $\mu$ l of 200  $\mu$ g/ml pDNA in 5% dextrose was mixed with an equal volume of DOTMA/Chol liposomes at 1160  $\mu$ g/ml and incubated for 30 min. For SCR lipoplex preparation, part of the 5% dextrose in the pDNA solution was replaced with saline and adjusted to the final NaCl concentration as indicated before mixing with liposome solution. The mixing ratio of liposomes and pDNA was expressed as a +/- charge ratio, which is the molar ratio of cationic lipids to pDNA phosphate residues [15]. A charge ratio of unity was obtained with 2.52  $\mu$ g total lipid/ $\mu$ g pDNA for DOTMA/Chol liposomes. The particle size of the lipoplex was measured using a dynamic light scattering spectrophotometer (LS-900, Otsuka Electronics, Osaka, Japan). The zeta potential of the lipoplex was determined with a laser electrophoresis zeta-potential analyzer (Zetasizer Nano ZS, Malvern Instruments Ltd., Worcestershire, UK).

### Fluorescent resonance energy transfer (FRET) analysis

FRET analysis was previously used for assessment of the stability of non-viral gene vectors by Itaka *et al.* [16]. Liposomes were labeled with two types of fluorescent lipid, NBD-DOPE or Rh-DOPE, at 2% (mol/mol) total lipid concentration. The fluorescence intensity spectra were measured using a spectrofluorophotometer (RF540, Shimadzu Co., Kyoto, Japan). The excitation wavelengths were 460 and 550 nm for NBD-DOPE and Rh-DOPE. The FRET from NBD-liposomes to Rh-liposomes was measured as a liposome-liposome interaction.

### In vivo gene expression experiments

Female 5-week-old ICR mice (20–23 g) were purchased from the Shizuoka Agricultural Cooperative Association for Laboratory Animals (Shizuoka, Japan). All animal experiments were carried out in accordance with the Principles of Laboratory Animal Care as adopted and promulgated by the US National Institutes of Health and the Guidelines for Animal Experiments of Kyoto University. Conventional or SCR lipoplex was administered intravenously (15, 23, 30, or 50  $\mu$ g pDNA/300  $\mu$ l). For the *in vivo* transfection experiments, liver, lung, or kidney was excised at 3, 6, or 96 h after injection. Each sample was homogenized with lysis buffer (0.1 M Tris/HCl containing 0.05% Triton X-100 and 2 mM EDTA (pH 7.8)). After three cycles of freeze/thawing, the homogenates were centrifuged at 10 000 g for 10 min at 4 °C. Then, 20  $\mu$ l of each supernatant were mixed with 100  $\mu$ l luciferase assay solution (Picagene, Toyo Ink Mfg. Co., Tokyo, Japan) and the light produced was immediately measured using a luminometer (Lumat LB 9507, Berthold Technologies, GmbH & Co., Bad Wildbad, Germany). The luciferase activity is given as the relative

number of light units (RLU) per mg protein. The protein content of the samples was determined using a protein quantification kit (Dojindo Molecular Technologies Inc., Gaithersburg, MD, USA).

### Alanine aminotransferase (ALT) activity

Conventional or SCR lipoplex was administered i.v. (30 or 50  $\mu$ g pDNA/300  $\mu$ l). Blood was collected from the vena cava, and mice were killed at 24 h. Then, ALT activity in plasma was determined by the UV-rate method using a Transaminase CII-test Wako kit (Wako Pure Chemicals Industry, Ltd., Osaka, Japan).

### TNF $\alpha$ concentration

Blood was collected from mice at 3 h after i.v. administration of lipoplex. The blood was allowed to coagulate for 3 h at 4 °C and serum was isolated as the supernatant fraction following the centrifugation. The serum samples were immediately stored at -80 °C until the enzyme-linked immunosorbent assay (ELISA). The amounts of TNF $\alpha$  in the serum were analyzed using ELISA kits (BD Biosciences Pharmingen, San Diego, CA, USA) according to the manufacturer's protocols.

### Statistical analysis

Statistical comparisons were performed by Student's t-test for two groups, and one-way analysis of variance (ANOVA) for multiple groups.  $P < 0.05$  was considered to be indicative of statistical significance.

## Results

### Possibility of enhanced gene expression of the SCR lipoplex

Figure 1 shows the transfection activity of the conventional lipoplex and the SCR lipoplex (5, 10, and 20 mM NaCl solution in lipoplex) after i.v. administration in mice. The transfection activity of the SCR lipoplex in lung was higher than that for the conventional lipoplex; in particular, the SCR lipoplex at 10 mM NaCl solution exhibited the highest transfection activity (Figure 1A). After i.v. administration of SCR lipoplex, the gene expression in the lung was approximately 100-fold higher than that found in the other organs (Figure 1B). Therefore, the SCR lipoplex at 10 mM NaCl solution was selected for evaluating the physicochemical and gene expression characteristics in the following experiments.

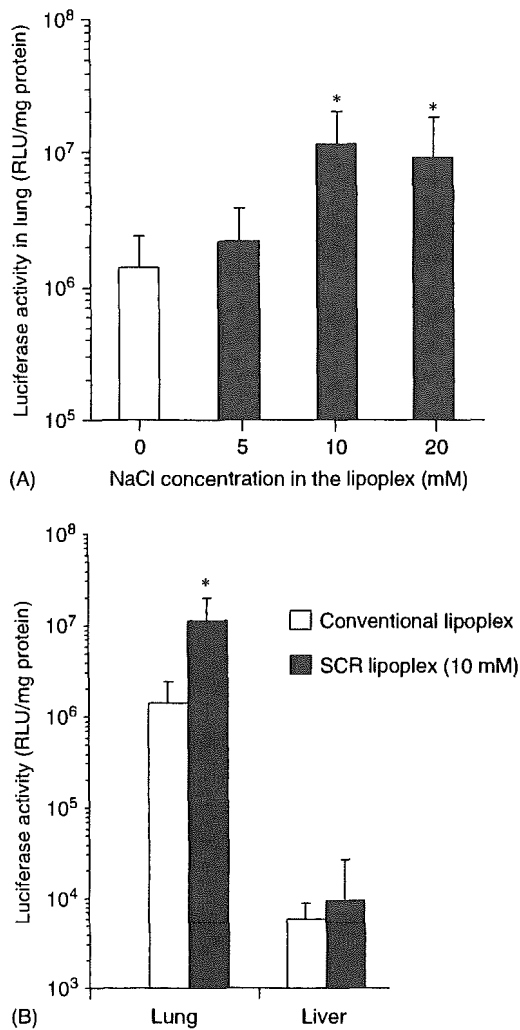


**Figure 1.** Enhanced hepatic transfection activity after intravenous (i.v.) administration of the SCR lipoplex in mice. (A) Effect of NaCl concentration of the lipoplex solution on the hepatic gene transfection activity by the SCR lipoplex. Lipoplexes were prepared at a charge ratio (-/+) of 1.0:3.1. Statistically significant differences (\* $P < 0.05$ ) compared with conventional lipoplex. (B) Comparison of gene expression in lung and liver after i.v. administration of the SCR lipoplex in mice. Lipoplexes were prepared at a charge ratio (-/+) of 1.0:3.1. Luciferase activity was determined 6 h post-injection of lipoplex. Each value represents the mean + standard deviation (SD) of at least three experiments

### Mean diameter, zeta potential, FRET analysis, and stability in saline of the SCR lipoplex

When the NaCl concentration was 5 mM, the mean particle sizes of the SCR lipoplexes were significantly reduced (Figure 2A). At NaCl concentrations of 10 mM, the particle sizes of the SCR lipoplexes were compatible with those of conventional lipoplex. When the NaCl concentration was 20 mM, the mean particle sizes of the SCR lipoplexes were significantly increased. The zeta potentials of the SCR lipoplex (10 mM) and the

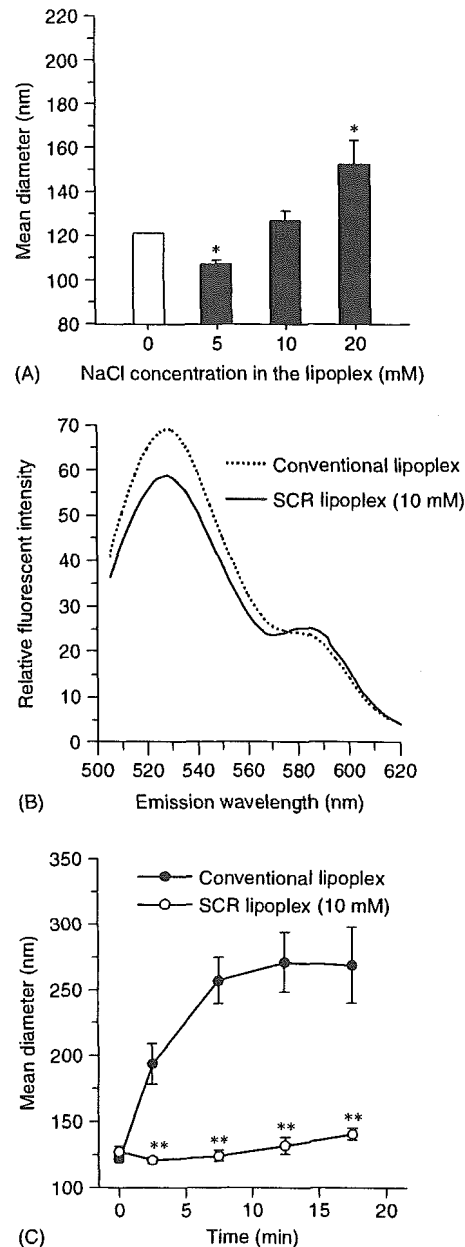


**Figure 2.** (A) Difference in particle size of the SCR lipoplex. The particle size of the SCR lipoplex was measured by dynamic light scattering spectrophotometry. Lipoplexes were prepared at a charge ratio (-/+) of 1.0:3.1. Each bar represents the mean diameter +SD of three experiments. Statistically significant differences (\* $P < 0.05$ ) compared with the conventional lipoplex. (B) FRET analysis of SCR lipoplex (10 mM NaCl) formation for the analysis of the liposome-liposome interaction. NBD-liposomes and Rh-liposomes were mixed at a ratio of 1:1 prior to lipoplex formation. Thirty minutes after mixing pDNA with a mixture of NBD- and Rh-labeled liposomes, the fluorescence intensity spectra were measured at an excitation wavelength of 460 nm. Lipoplexes were prepared at a charge ratio (-/+) of 1.0:3.1. Similar results were obtained in two other independent runs. (C) Stability of the SCR lipoplex (10 mM NaCl) after mixing with saline as a model of physiological conditions. Lipoplexes were prepared at a charge ratio (-/+) of 1.0:3.1. Each value represents the mean diameter  $\pm$ SD of three experiments. Statistically significant differences (\*\* $P < 0.01$ ) compared with the conventional lipoplex

conventional lipoplex were  $57.1 \pm 4.22$  and  $64.5 \pm 0.65$  mV ( $N = 3$ ,  $P < 0.01$ ).

FRET analysis was performed to further evaluate the formation of SCR lipoplex (10 mM) (Figure 2B). The FRET effect was evaluated using the peak ratio of nitrobenzoxadiazole (NBD) and rhodamine (Rh). Using these lipids, the changes in the liposome–liposome interaction of the SCR lipoplex using NBD- and Rh-labeled liposomes were measured. Distinct energy transfer from NBD (emission 534 nm) to Rh (emission 590 nm) was observed and the NBD/Rh fluorescence intensity ratios ( $F_{534}/F_{590}$ ) were  $3.3 \pm 0.2$  ( $N = 3$ ) and  $2.2 \pm 0.2$  ( $N = 3$ ) for 0 and 10 mM NaCl solutions, respectively, suggesting that each cationic liposome in the SCR lipoplex had easier access to the others than the conventional lipoplex (0 mM NaCl solution). Statistically significant differences were observed between the SCR lipoplex (10 mM NaCl) and the conventional lipoplex ( $P < 0.01$ ). Thus, pDNA in the SCR lipoplex may be covered by many cationic liposomes; such behavior of the SCR lipoplex is expected to enhance the stability of pDNA. These results for the size change and FRET analysis corresponded to those in our previous report involving the galactosylated SCR lipoplex [11].

When conventional lipoplex was diluted with saline, the mean particle size was greatly increased as time advanced (Figure 1C). In contrast, the SCR lipoplex (10 mM NaCl) delayed the particle size enlargement, indicating SCR lipoplexes were more stable than the conventional lipoplex.

### Gene expression characteristics of the SCR lipoplex

At charge ratios (-/+) of 1.0:2.3 and 1.0:3.1, the gene expression of the SCR lipoplex was significantly higher than that of the conventional lipoplex (Figure 3A). At doses ranging from 15 to 30  $\mu$ g, the gene expression of the SCR lipoplex was significantly higher than that of the conventional lipoplex (Figure 3B). As for the gene expression periods, the SCR lipoplex maintained significantly higher transfection activity until 4 days than that of the conventional lipoplex (Figure 4).

### Biodistribution characteristics of the SCR lipoplex

Figure 5 shows the distribution of the SCR and the conventional lipoplex following i.v. administration in mice at 30 min. Most of the radioactivity accumulated in the lung or liver. However, the lung accumulation of the SCR lipoplex was significantly higher than that of the conventional lipoplex.

### Liver toxicity of the SCR lipoplex

In order to confirm the toxicity of the SCR lipoplex, ALT activity in serum was measured as an index of liver

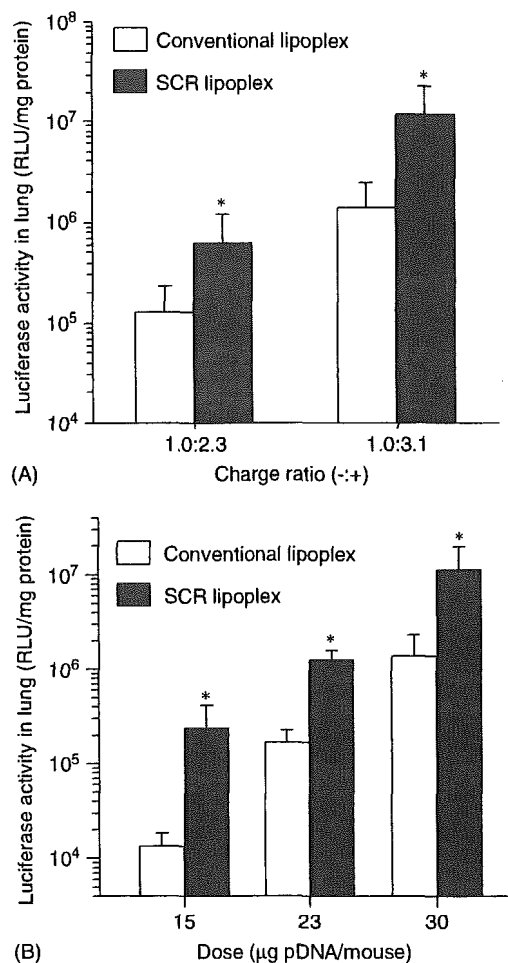


Figure 3. (A) Effect of charge ratio on the transfection activity of the SCR lipoplex in lung. Lipoplexes were prepared at charge ratios (-/+) of 1.0:2.3 and 1.0:3.1. Each value represents the mean diameter  $\pm$ SD of three experiments. Statistically significant differences ( $*P < 0.05$ ) compared with the conventional lipoplex. (B) Effect of pDNA dose on the transfection activity of the SCR lipoplex in lung. Lipoplexes were prepared at a charge ratio (-/+) of 1.0:3.1. Each value represents the mean diameter  $\pm$ SD of three experiments. Statistically significant differences ( $*P < 0.05$ ) compared with the conventional lipoplex

toxicity. When the gene expression levels of the SCR lipoplex and the conventional lipoplex were compared, the SCR lipoplex at a dose of 30  $\mu$ g was comparable with that of the conventional lipoplex at a dose of 50  $\mu$ g (Figure 6A). A significantly higher ALT activity was observed with the conventional lipoplex (pDNA dose: 50  $\mu$ g), but not with the SCR lipoplex (pDNA dose: 30  $\mu$ g). Similarly,  $TNF\alpha$  concentration of the conventional lipoplex (pDNA dose: 50  $\mu$ g) was significantly higher than that of the SCR lipoplex (pDNA dose: 30  $\mu$ g).

### Discussion

In the present study, DOTMA/Chol liposomes were selected as cationic liposomes for intravenous (i.v.)

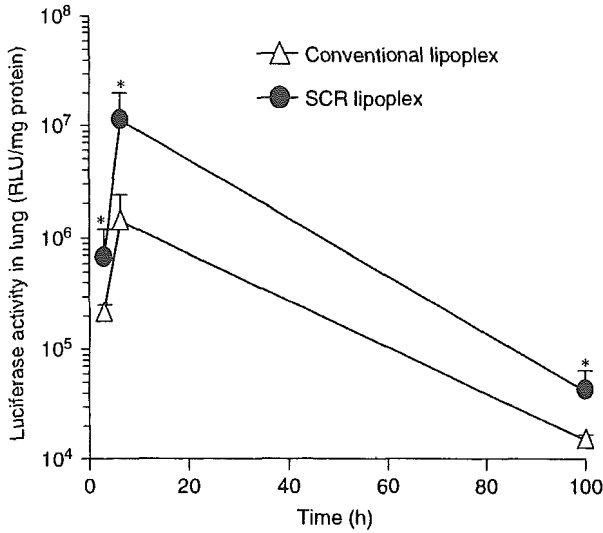


Figure 4. Time-course of the gene expression in lung after intravenous administration of the SCR lipoplex in mice. Luciferase activity was determined 6 h, 12 h, and 3 days post-injection of the SCR lipoplex. Lipoplexes were prepared at a charge ratio (-/+) of 1.0:3.1. Each value represents the mean + SD of at least three experiments. Statistically significant differences (\**P* < 0.05) compared with the conventional lipoplex

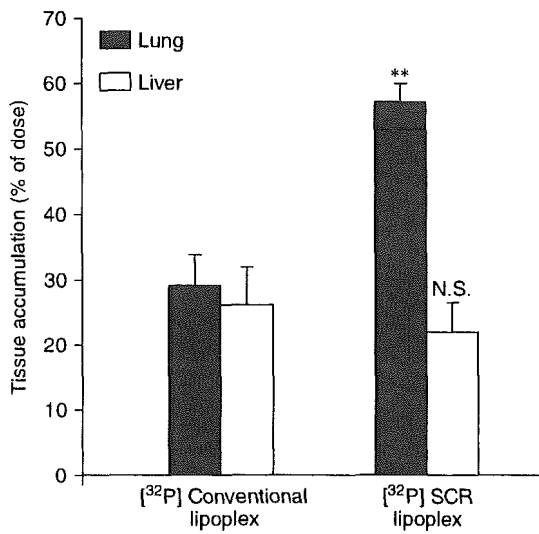


Figure 5. Biodistribution characteristics in lung, liver, and kidney after intravenous administration of the SCR lipoplex in mice. Radioactivity was determined 30 min post-injection of lipoplex. Lipoplex were prepared at a charge ratio (-/+) of 1.0:3.1. Each value represents the mean + SD of at least three experiments. Statistically significant differences (\*\**P* < 0.01) compared with the conventional lipoplex. N.S.; Not significant

administration because of their high transfection activity [6,12,13]. Despite the fact that the concept of transfecting with lipoplex is quite simple, we need to further improve the transfection efficacy, and evaluate potential toxicity in the case of clinical application.

Although there are some current methodologies for stabilizing non-viral carriers, each method has the

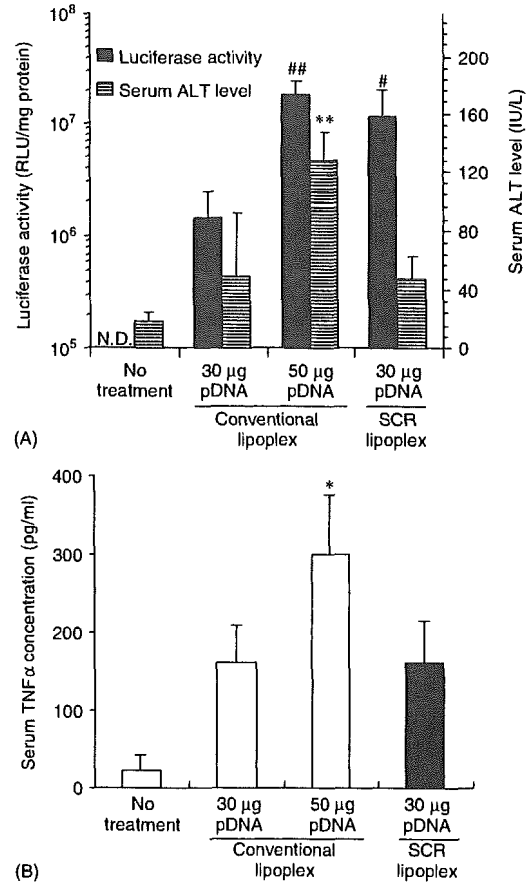


Figure 6. Gene expression and ALT activity after intravenous (i.v.) administration of the SCR lipoplex in mice (A). Luciferase activity and ALT activity were determined 6 and 24 h post-injection of the SCR lipoplex. Lipoplexes were prepared at a charge ratio (-/+) of 1.0:3.1. Each value represents the mean + SD of at least three experiments. Statistically significant differences (\*\**P* < 0.01 (luciferase activity), #*P* < 0.05, ##*P* < 0.01 (ALT activity)) compared with the conventional lipoplex. TNFα concentration after i.v. administration of the SCR lipoplex in mice (B). TNFα concentrations were determined 3 h post-injection of the SCR lipoplex. Lipoplexes were prepared at a charge ratio (-/+) of 1.0:3.1. Each value represents the mean + SD of at least three experiments. Statistically significant differences (\**P* < 0.05) compared with the SCR lipoplex

disadvantage of affecting the transfection efficiency. In most cases, PEGylated lipids were used to stabilize the lipoplex; however, the surface modification of liposomes with PEG results in a reduced interaction with cells so that the system exhibits a low transfection potential [17,18]. For the ideal design of gene carrier systems, the lipoplex needs to be stabilized without any loss of transfection activity. In the present study, we have demonstrated the possibility of a novel method of stabilizing the lipoplex to enhance the transfection activity by using NaCl for complex formation.

Lipoplexes for *in vivo* gene delivery are generally prepared in non-ionic solution (i.e., dextrose) because the lipoplex form aggregates in the presence of isotonic concentrations of ionic solutions such as saline (150 mM NaCl). In the present study, we hypothesized that the

presence of an essential amount of NaCl during lipoplex formation would regulate the repulsion between cationic liposomes and the fusion of the cationic liposomes in the lipoplex would be accelerated by partial neutralization of the positive charge on the surface of the cationic liposomes. This hypothesis was confirmed, in part, by the results of the FRET analysis (Figure 2B) and zeta potential measurements, i.e., moderate neutralization of the positive charge on the surface of cationic liposomes by an essential concentration of NaCl can ensure sufficient repulsion of the lipoplex intermediates. Since the fusion of each cationic liposome was enhanced, cationic lipids may extensively cover pDNA in the SCR lipoplex. These observations correspond to our previous observations in the galactosylated SCR lipoplex used for hepatocyte-selective gene expression [10]; consequently, SCR theory can be applied to different types of lipoplex.

The distribution characteristics during the early periods are important for gene expression. In fact, Barron *et al.* demonstrated that lipoplex-mediated gene expression to the lung occurs within 60 min after i.v. administration [19]. To investigate the mechanism of the enhanced gene expression by the SCR lipoplex, a distribution study was performed using [<sup>32</sup>P]-labeled pDNA. After i.v. administration, approximately 30% of the [<sup>32</sup>P] conventional lipoplex was distributed in the lung at 30 min (Figure 5). This result is similar to that reported by Li and Huang involving a distribution study by a liposome-protamine-[<sup>125</sup>I]DNA (LPD) complex [15]. In contrast, approximately 60% of the [<sup>32</sup>P] SCR lipoplex was distributed in the lung at 30 min, indicating that pDNA in the SCR lipoplex accumulates more efficiently in the lung. Hence, the higher gene expression in the lung can be ascribed to the difference in distribution between the conventional lipoplex and the SCR lipoplex.

As shown in Figure 1B, gene expression levels were enhanced in the lung, but were not enhanced in liver and kidney by the SCR lipoplex. This observation agrees with the distribution study showing that SCR lipoplexes were only efficiently distributed in the lung after i.v. administration (Figure 5). It has been reported that *in vivo* gene expression levels are greatly affected by the charge ratio (-/+ ) of the lipoplex and the pDNA dose [3,6,7]. In order to further confirm the transfection activity by SCR lipoplexes, the charge ratio and/or pDNA dose were also varied and the effect of these factors was analyzed. At charge ratios (-/+ ) of 1.0:2.3 and 1.0:3.1, the gene expression of the SCR lipoplex was significantly higher than that of the conventional lipoplex (Figure 3A). Similarly, at pDNA doses ranging from 15 to 30 µg, the gene expression of the SCR lipoplex was always significantly higher than that of the conventional lipoplex (Figure 3B). These results indicate that the SCR lipoplex method could enhance gene expression in lung, irrespective of the charge ratio and/or the pDNA dose.

For the clinical application of the lipoplex, toxicity is an important factor. Even if the gene expression is at a favorable level, severe toxicity could mean that clinical application is impossible. Li *et al.* reported

that, although a cationic lipid/protamine/DNA complex showed higher gene expression in lung, it induced high levels of inflammatory cytokines [20]. As for the toxicity of the lipoplex, Loisel *et al.* systemically analyzed and reported that the i.v. administration of lipoplex does not induce any toxic effects in the lung, but liver toxicity was observed as reflected in the serum transaminase levels [21]. To confirm the effect of toxicity on SCR lipoplex administration, we evaluated the ALT activity as an index of liver damage. Although the gene expression of the SCR lipoplex at a dose of 30 µg was comparable with that of conventional lipoplex at a dose of 50 µg, a significantly higher ALT activity was observed by the conventional lipoplex at a dose of 50 µg (Figure 6A). Similarly, serum TNFα concentration of the conventional lipoplex at a dose of 50 µg was significantly higher than that of the SCR lipoplex at a dose of 30 µg (Figure 6B). This result corresponds to the observation of the ALT activity in Figure 6A. These results lead us to believe that the SCR lipoplex could enhance the gene expression in lung without the liver toxicity. Tousignant *et al.* [22] suggested that the hepatic damage was induced by the cytokines from Kupffer cells because of marked accumulation of lipoplex following i.v. administration. Similarly, we previously reported that, following the administration of lipoplex, inflammatory cytokines were released from Kupffer cells in the liver [23]. Therefore, this result may be explained by the fact that the liver (Kupffer cells) accumulation of SCR lipoplex was as same as that of the conventional lipoplex (Figure 5).

So far, some trials have been carried out to reduce the release of inflammatory cytokines. Recently, Tan *et al.* reported that the sequential injection of cationic liposomes and pDNA effectively transfects the lung with only minimal inflammatory toxicity [24]. However, sequential injection is complicated and this may include (i) a need for two administrations and (ii) consideration of the time of administration. Reducing the CpG sequence number in pDNA is another method to reduce the cytokine release [25]. However, an important part of the CpG sequence in pDNA cannot be removed because of the reduced transfection efficacy. Therefore, another approach to reduce the toxicity is also required for the safe use of lipoplexes in humans. Since the SCR lipoplex enhances gene expression in lung (Figures 3 and 6), the pDNA dose could be reduced to obtain the essential level of gene expression for therapy; consequently, the toxicity would be reduced.

We previously reported that the hepatic transfection activity of a galactosylated SCR lipoplex dispersed by 5 mM NaCl solution was about 2-fold higher than that of 10 mM NaCl solution in mice [10]. In the present study, we demonstrated that a SCR lipoplex dispersed by 10 mM NaCl solution was about 5-fold more active than that obtained by 5 mM NaCl solution in mice. The optimal concentration of NaCl is different in these studies. This could be explained by the difference in the site of the target cells. In *in vivo* [8] and *in situ* [26] studies, we previously demonstrated that the penetration of the

galactosylated lipoplex through the hepatic fenestrated endothelium to the parenchymal cells was greatly restricted. Previous results showed that the size of the galactosylated SCR lipoplex in 5 mM NaCl solution was smaller than that of a conventional galactosylated lipoplex [10]. The size reduction of the SCR lipoplex in 5 mM NaCl solution was also confirmed in the present study. In contrast, the access to lung endothelial cells is not restricted by the size of the lipoplex. Taking these factors into consideration, the site of the target cells could be considered for the effective application of the SCR theory.

In conclusion, we demonstrated enhanced transfection activity in the lung by stabilized lipoplex using NaCl for complex formation. FRET analysis revealed that the NaCl solution in the lipoplex enhanced the fusion of cationic liposomes in the lipoplex; consequently, the *in vivo* transfection was greatly enhanced without affecting liver toxicity. Pharmacokinetic studies demonstrated higher lung accumulation of the SCR lipoplex. This distribution characteristic partly explains the mechanism of enhanced *in vivo* transfection efficacy in the lung by the SCR lipoplex. Also, our data indicated the importance of the ionic concentration in the lipoplex solution for gene expression. The information we obtained will be of great value for the future use, design, and development of lipoplexes for *in vivo* applications.

## Acknowledgements

This work was supported in part by Grant-in-Aids for Scientific Research from the Ministry of Education, Culture, Sports, Science, and Technology of Japan, by Health and Labour Sciences Research Grants for Research on Advanced Medical Technology from the Ministry of Health, Labour and Welfare of Japan, and by the 21st Century COE Program "Knowledge Information Infrastructure for Genome Science".

## References

- Zhu N, Liggitt D, Liu Y, Debs R. Systemic gene expression after intravenous DNA delivery into adult mice. *Science* 1993; **261**: 209–211.
- Wheeler CJ, Felgner PL, Tsai YJ, *et al.* A novel cationic lipid greatly enhances plasmid DNA delivery and expression in mouse lung. *Proc Natl Acad Sci U S A* 1996; **93**: 11 454–11 459.
- Liu F, Qi H, Huang L, Liu D. Factors controlling the efficiency of cationic lipid-mediated transfection *in vivo* via intravenous administration. *Gene Ther* 1997; **4**: 517–523.
- Hong K, Zheng W, Baker A, Papahadjopoulos D. Stabilization of cationic liposome-plasmid DNA complexes by polyamines and poly(ethylene glycol)-phospholipid conjugates for efficient *in vivo* gene delivery. *FEBS Lett* 1997; **400**: 233–237.
- Sakurai F, Nishioka T, Saito H, *et al.* Interaction between DNA-cationic liposome complexes and erythrocytes is an important factor in systemic gene transfer via the intravenous route in mice: the role of the neutral helper lipid. *Gene Ther* 2001; **8**: 677–686.
- Song YK, Liu F, Chu S, Liu D. Characterization of cationic liposome-mediated gene transfer *in vivo* by intravenous administration. *Hum Gene Ther* 1997; **8**: 1585–1594.
- Hofland HE, Nagy D, Liu JJ, *et al.* *In vivo* gene transfer by intravenous administration of stable cationic lipid/DNA complex. *Pharm Res* 1997; **14**: 742–749.
- Kawakami S, Fumoto S, Nishikawa M, Yamashita F, Hashida M. *In vivo* gene delivery to the liver using novel galactosylated cationic liposomes. *Pharm Res* 2000; **17**: 306–313.
- Kawakami S, Yamashita F, Nishida K, Nakamura J, Hashida M. Glycosylated cationic liposomes for cell-selective gene delivery. *Crit Rev Ther Drug Carrier Syst* 2002; **19**: 171–190.
- Fumoto S, Kawakami S, Ito Y, Shigeta K, Yamashita F, Hashida M. Enhanced hepatocyte-selective *in vivo* gene expression by stabilized galactosylated liposome/plasmid DNA complex using sodium chloride for complex formation. *Mol Ther* 2004; **10**: 719–729.
- Sambrook J, Fritsch EF, Maniatis T. *Molecular Cloning: A Laboratory Manual* (2nd edn). Cold Spring Harbor Laboratory Press: Plainview, NY, 1989.
- Kawakami S, Sato A, Yamada M, Yamashita F, Hashida M. The effect of lipid composition on receptor-mediated *in vivo* gene transfection using mannosylated cationic liposomes in mice. *ST P Pharma Sci* 2001; **11**: 117–120.
- Sakurai F, Terada T, Maruyama M, *et al.* Therapeutic effect of intravenous delivery of lipoplexes containing the interferon- $\beta$  gene and poly I: poly C in a murine lung metastasis model. *Cancer Gene Ther* 2003; **10**: 661–668.
- Kawakami S, Harada A, Sakanaka K, *et al.* *In vivo* gene transfection via intravitreal injection of cationic liposome/plasmid DNA complexes in rabbits. *Int J Pharm* 2004; **278**: 255–262.
- Li S, Huang L. *In vivo* gene transfer via intravenous administration of cationic lipid-protamine-DNA (LPD) complexes. *Gene Ther* 1997; **4**: 891–900.
- Itaka K, Harada A, Nakamura K, Kawaguchi H, Kataoka K. Evaluation by fluorescence resonance energy transfer of the stability of nonviral gene delivery vectors under physiological conditions. *Biomacromolecules* 2002; **3**: 841–845.
- Harvie P, Wong FM, Bally MB. Use of poly(ethylene glycol)-lipid conjugates to regulate the surface attributes and transfection activity of lipid-DNA particles. *J Pharm Sci* 2000; **89**: 652–663.
- Song LY, Ahkong QF, Rong Q, *et al.* Characterization of the inhibitory effect of PEG-lipid conjugates on the intracellular delivery of plasmid and antisense DNA mediated by cationic lipid liposomes. *Biochim Biophys Acta* 2002; **1558**: 1–13.
- Barron LG, Gagne L, Szoka FC Jr. Lipoplex-mediated gene delivery to the lung occurs within 60 minutes of intravenous administration. *Hum Gene Ther* 1999; **10**: 1683–1694.
- Li S, Wu SP, Whitmore M, *et al.* Effect of immune response on gene transfer to the lung via systemic administration of cationic lipidic vectors. *Am J Physiol* 1999; **276**: L796–L804.
- Loisel S, Le Gall C, Doucet L, Ferec C, Floch V. Contribution of plasmid DNA to hepatotoxicity after systemic administration of lipoplexes. *Hum Gene Ther* 2001; **12**: 685–696.
- Tousignant JD, Gates AL, Ingram LA, *et al.* Comprehensive analysis of the acute toxicities induced by systemic administration of cationic lipid : plasmid DNA complexes in mice. *Hum Gene Ther* 2000; **11**: 2493–2513.
- Sakurai F, Terada T, Yasuda K, Yamashita F, Takakura Y, Hashida M. The role of tissue macrophages in the induction of proinflammatory cytokine production following intravenous injection of lipoplexes. *Gene Ther* 2002; **9**: 1120–1126.
- Tan Y, Liu F, Li Z, Li S, Huang L. Sequential injection of cationic liposome and plasmid DNA effectively transfects the lung with minimal inflammatory toxicity. *Mol Ther* 2001; **3**: 673–682.
- Yew NS, Zhao H, Przybylska M, *et al.* CpG-depleted plasmid DNA vectors with enhanced safety and long-term gene expression *in vivo*. *Mol Ther* 2002; **5**: 731–738.
- Fumoto S, Nakadori F, Kawakami S, Nishikawa M, Yamashita F, Hashida M. Analysis of hepatic disposition of galactosylated cationic liposome/plasmid DNA complexes in perfused rat liver. *Pharm Res* 2003; **20**: 1452–1459.

# Effect of Galactose Density on Asialoglycoprotein Receptor-Mediated Uptake of Galactosylated Liposomes

CHITTIMA MANAGIT, SHIGERU KAWAKAMI, FUMIYOSHI YAMASHITA, MITSURU HASHIDA

Department of Drug Delivery Research, Graduate School of Pharmaceutical Sciences, Kyoto University, Sakyo-ku, Kyoto, 606-8501, Japan

Received 18 February 2005; revised 5 May 2005; accepted 19 May 2005

Published online 31 August 2005 in Wiley InterScience (www.interscience.wiley.com). DOI 10.1002/jps.20443

**ABSTRACT:** Galactosylated (Gal) liposomes containing various molar ratios of cholesterol-5-yloxy-*N*-(4-((1-imino-2-D-thiogalactosylethyl)formamide (Gal-C4-Chol) as a ligand for asialoglycoprotein receptors were prepared to study the effect of the galactose content of Gal-liposomes labeled with [<sup>3</sup>H]cholesteryl hexadecyl ether on their targeted delivery to hepatocytes. The uptake characteristics of Gal-liposomes having Gal-C4-Chol of 1.0%, 2.5%, 3.5%, 5.0%, and 7.5% were evaluated. The uptake and internalization by HepG2 cells was enhanced by the addition of Gal-C4-Chol to the Gal-liposomes. In the presence of excess galactose, the uptake of Gal-liposomes having Gal-C4-Chol of 3.5%, 5.0%, and 7.5% was inhibited suggesting asialoglycoprotein receptor mediated uptake. After intravenous injection, Gal-liposomes having Gal-C4-Chol of 3.5%, 5.0%, and 7.5%, rapidly disappeared from the blood and exhibited rapid liver accumulation with up to about 80% of the dose within 10 min whereas Gal-liposomes having low Gal-C4-Chol (1.0% and 2.5%) showed a slight improvement in liver accumulation compared with bare-liposomes. Gal-liposomes with high Gal-C4-Chol are preferentially taken up by hepatocytes and the highest uptake ratio by parenchymal cells (PC) and nonparenchymal cells (NPC) (PC/NPC ratio) was observed with Gal-liposomes having of 5.0% Gal-C4-Chol. We report here that the galactose density of Gal-liposomes prepared by Gal-C4-Chol is important for both effective recognition by asialoglycoprotein receptors and cell internalization.

© 2005 Wiley-Liss, Inc. and the American Pharmacists Association J Pharm Sci 94:2266–2275, 2005

**Keywords:** drug delivery system; site-specific delivery; targeting; targeted drug delivery; galactosylated liposomes; liposomes; lipids; asialoglycoprotein receptors; hepatocytes; pharmacokinetics

## INTRODUCTION

Receptor-mediated drug delivery is a promising approach to site-selective drug delivery. Receptors for carbohydrates, such as the asialoglycoprotein receptor on hepatocytes (liver parenchymal cells) and the mannose receptor on several macrophages and liver endothelial cells, recognize the corresponding sugars on the nonreducing term-

inal of sugar chains.<sup>1</sup> Among these sugar-recognized receptors, asialoglycoprotein receptors on hepatocytes have been found to be one of the most promising candidate targets in many drug carrier studies since they exhibit high affinity and a rapid internalization rate.<sup>2</sup>

The receptor-ligand interaction is known to show a significant “cluster effect” in which a multivalent interaction results in extremely strong binding of ligand to the receptors.<sup>3</sup> We have already demonstrated that the *in vivo* recognition of galactosylated macromolecules by asialoglycoprotein receptors correlates with the degree of galactose modification.<sup>4</sup> A pharmacokinetic analysis of the tissue disposition patterns of galactose

Correspondence to: Mitsuru Hashida (Telephone: +81-75-753-4525; Fax: +81-75-753-4575; E-mail: hashidam@pharm.kyoto-u.ac.jp)

Journal of Pharmaceutical Sciences, Vol. 94, 2266–2275 (2005)  
© 2005 Wiley-Liss, Inc. and the American Pharmacists Association

units on the protein surface determines the affinity of galactosylated proteins for asialoglycoprotein receptor-mediated hepatic uptake.<sup>4</sup> These results indicate that the drug targeting efficacy to hepatocytes using galactosylated macromolecular carriers is dependent on the galactose modification.

To date, various natural and synthetic galactosylated derivatives have been developed as ligands for asialoglycoprotein receptors.<sup>5-7</sup> For successful liposomal targeting, the chemical structure and physicochemical properties of glycolipids are crucial. As far as the ligand design of glycolipids is concerned, both the number of galactose moieties and the types of hydrophobic anchor are important. Since highly lipophilic compounds are more stably incorporated into the liposomal membrane,<sup>8</sup> introduction of mono-antennary galactoside to the lipids is more appropriate. In addition, the synthesis of mono-antennary galactoside is simpler than that of multi-antennary galactoside.

Taking these factors into considerations, we previously synthesized a galactosylated cholesterol derivative, cholesten-5-yloxy-*N*-(4-((1-imino-2-D-thiogalactosylethyl)formamide (Gal-C4-Chol), having cholesterol for stable incorporation into liposomes, and a mono-antennary galactoside for recognition by the asialoglycoprotein receptors.<sup>9</sup> In this previous study, we reported that Gal-C4-Chol combining with neutral lipids (DSPC and Chol) was taken up by the liver parenchymal cells by asialoglycoprotein receptor-mediated uptake.<sup>10,11</sup> However, in order to ensure hepatocyte-specific targeting of liposomes by galactosylation, the galactose density on the liposomal surface needs to be controlled.

To understand the effects of the galactose density on the liposomal surface on the targeting efficiency of galactosylated liposomes to hepatocytes, galactosylated liposomes (Gal-liposomes) having different Gal-C4-Chol molar ratios were prepared. Then, the *in vitro* uptake characteristics of the Gal-liposomes were investigated in human hepatoma HepG2 cells, which are known to express asialoglycoprotein receptors. Moreover, we examined the tissue disposition and intrahepatic (i.e., to hepatocytes or liver nonparenchymal cells (NPC)) distribution characteristics of Gal-liposomes after intravenous administration into mice. These galactosylated liposomes were radiolabeled with [<sup>3</sup>H]cholesteryl hexadecyl ether (CHE).<sup>12</sup> We report here that the galactose density of Gal-liposomes prepared by Gal-C4-Chol is important for both efficient recognition by asialoglycoprotein receptors and cell internalization.

## MATERIALS AND METHODS

### Materials

*N*-(4-aminobutyl)carbamic acid tert-butyl ester was purchased from Tokyo Chemical Industry Co. (Tokyo, Japan). Distearoyl-L-phosphatidylcholine (DSPC) and cholesteryl chloroformate were purchased from Sigma Chemical Co. (St. Louis, MO). Cholesterol (Chol) and Clear-Sol I were obtained from Nacalai Tesque, Inc. (Kyoto, Japan). Galactose was obtained from Wako Pure Chemical Co. (Kyoto, Japan). Soluene 350 was purchased from Packard Bioscience Co. (Groningen, The Netherlands). [<sup>3</sup>H]cholesteryl hexadecyl ether (CHE) was purchased from NEN Life Science Products, Inc. (Boston, MA). Dulbecco's modified Eagle's minimum essential medium (DMEM) was obtained from Nissui Pharmaceutical Co. (Tokyo, Japan). 2-imino-2-methoxyethyl-1-thiogalactoside (IME-thiogalactoside) was synthesized as reported previously.<sup>13</sup> All other chemicals were of the highest purity commercially available.

### Synthesis of Gal-C4-Chol

Gal-C4-Chol was synthesized by the method described previously.<sup>9</sup> Briefly, cholesteryl chloroformate was reacted with *N*-(4-aminobutyl)carbamic acid tert-butyl ester in chloroform for 24 h at room temperature and then incubated with trifluoroacetic acid for 4 h at 4°C. *N*-(4-aminobutyl)-(cholesten-5-yloxy)formamide was obtained after evaporation of the solvent. A quantity of the resultant material was added to an excess of 2-imino-2-methoxyethyl-1-thiogalactoside in pyridine containing triethylamine.<sup>13</sup> After 24 h incubation at room temperature, the reaction mixture was evaporated, resuspended in water and dialyzed against distilled water for 48 h using a semi-permeable membrane (12 kDa cut-off). Finally, the dialyzate was lyophilized.

### Preparation of Liposomes

A mixture of DSPC and Chol, with or without Gal-C4-Chol, was dissolved in chloroform and evaporated to dryness in a round-bottomed flask. Then, the lipid film formed was resuspended in 5 mL sterile phosphate-buffered saline (pH 7.4). After hydration, the dispersion was sonicated for 3 min (200 W). Each resulting suspension was passed through a 200 nm (5-times) and 100 nm (5-times)



pore size polycarbonate membrane at 60°C using an extruder (Northern Lipids, Vancouver, Canada). The concentration of liposomes was adjusted to 5 mg/mL total lipids based on radioactivity measurement. Radiolabeling of liposomes was performed by addition of [<sup>3</sup>H]CHE (500 µCi) to the lipid mixture before formation of a thin film layer. The particle sizes of liposomes without radioisotope were measured in a dynamic light-scattering spectrophotometer (LS-900, Otsuka Electronics, Co., Ltd., Osaka, Japan). The zeta potential of liposome was determined with a laser electrophoresis zeta-potential analyzer (LEZA-500T, Otsuka Electronics).

### Lectin-Induced Aggregation of Liposomes

Liposomes (0.1 mg/mL total lipid) were incubated with 100 µL *Ricinus communis* agglutinin, RCA120 (1.0 mg/mL) in a cuvette. After rapid mixing, aggregation of the liposomes was estimated at room temperature by the time dependent increase in turbidity, as measured by the absorbance at 350 nm with a UV-3100 spectrometer (Shimadzu Co., Kyoto, Japan). The reversibility of the aggregation was assessed by the addition of 100 µL (10 mg/mL) free galactose.

### In Vitro Uptake Study

The HepG2 cells were plated on a 12-well cluster dish at a density of  $2 \times 10^5$  cells/3.8 cm<sup>2</sup> and cultivated in 800 µL DMEM supplemented with 10% fetal bovine serum (Invitrogen Co., Carlsbad, CA). Twenty-four hours later, the culture medium was replaced with an equivalent volume of HBSS containing [<sup>3</sup>H]liposomes (0.25 mg/mL, 1.8 kBq/mL). For the inhibition study, 20 mM galactose was added to the liposome solution. After incubation for 1 h at 37°C, the solution was removed by aspiration, and the cells were washed five times with ice-cold HBSS buffer. For separation of the internalized and surface bound liposomes, the cells were washed three times with acetate buffer (pH 4.0) to remove the liposomes bound to the cell surface. The cells were then solubilized in 0.5 mL 1M NaOH and the radioactivity was assayed using a liquid scintillation counter (LSA-500, Beckman, Tokyo, Japan). The protein content of each sample was determined by a modification of the Lowry method.<sup>14</sup> In another set of experiments, the cells were preincubated with HBSS containing 10 mM NaN<sub>3</sub> for 20 min prior to the addition of liposomes.

### In Vivo Distribution Study

Five-week-old male ddY mice (25.0–30.0 g) were obtained from Shizuoka Agricultural Co-operative Association for Laboratory Animals (Shizuoka, Japan). All animal experiments were carried out in accordance with the Principles of Laboratory Animal Care as adopted and promulgated by the US National Institutes of Health and the Guideline for Animal Experiments of Kyoto University. [<sup>3</sup>H]CHE (1.0 µCi/100 µL)-labeled liposomes were injected into the tail vein of mice at a dose of 25 mg/kg. At predetermined time points, blood was collected from the vena cava under anesthesia and mice were then sacrificed. The liver, kidney, spleen, heart, and lung were collected, washed with saline, blotted dry, and weighed. A complete urine collection was obtained by combining the excreted urine with that remaining in the bladder. Ten microliters blood, 200 µL of urine, and a small amount of each tissue were digested with 0.7 mL Soluene-350 by incubating the samples overnight at 45°C. Following digestion, 0.2 mL isopropanol, 0.2 mL 30% hydroperoxide, 0.1 mL 5N HCl, and 5.0 mL Clear-Sol I were added. The samples were stored overnight and the radioactivity was measured in a liquid scintillation counter (LSA-500, Beckman Coulter, Inc., Tokyo, Japan).

### Calculation of Organ Uptake Clearance

Tissue distribution data were evaluated using the organ clearances as reported previously.<sup>15–17</sup> Briefly, the tissue uptake rate can be described by the following equation:

$$\frac{dX_t}{dt} = CL_{\text{uptake}} \cdot C_b \quad (1)$$

where  $X_t$  is the amount of [<sup>3</sup>H]-labeled liposomes in the tissue at time  $t$ ,  $CL_{\text{uptake}}$  is the tissue uptake clearance, and  $C_b$  is the blood concentration of [<sup>3</sup>H]-labeled liposomes. Integration of Eq. 1 gives

$$X_t = CL_{\text{uptake}} \cdot \text{AUC}(0-t) \quad (2)$$

where  $\text{AUC}(0-t)$  represents the area under the blood concentration-time curve from time 0 to  $t$ . Eq. 2 divided by  $C_b$  gives

$$\frac{X_t}{C_b} = \frac{CL_{\text{uptake}} \cdot \text{AUC}(0-t)}{C_b} \quad (3)$$

The  $CL_{\text{uptake}}$  value can be obtained from the initial slope of a plot of  $X_t/C_b$  versus  $\text{AUC}(0-t)/C_b$ .

### Intrahepatic Distribution Study

The separation of liver parenchymal cells and nonparenchymal cells was performed by the collagenase perfusion method.<sup>18,19</sup> Briefly, mice were anesthetized with an intraperitoneal injection of pentobarbital sodium (40–60 mg/kg) and given an intravenous injection of [<sup>3</sup>H]CHE (0.5–1.0  $\mu$ Ci/100  $\mu$ L)-labeled liposomes. The body temperatures were kept at 37°C with a heat lamp during the experiment. Then, 30 min after administration, the liver was perfused first with Ca<sup>2+</sup>, Mg<sup>2+</sup>-free perfusion buffer (10 mM *N*-2-hydroxyethylpiperazine-*N'*-2-ethanesulfonic acid (HEPES), 137 mM NaCl, 5 mM KCl, 0.5 mM NaH<sub>2</sub>PO<sub>4</sub>, and 0.4 mM Na<sub>2</sub>HPO<sub>4</sub>, pH 7.2) for 10 min followed by perfusion buffer supplemented with 5 mM CaCl<sub>2</sub> and 0.05% (w/v) collagenase (type I; pH 7.5) for 10 min. As soon as the perfusion started, the vena cava and aorta were cut and the perfusion rate was maintained at 3–4 mL/min. Following the discontinuation of perfusion, the liver was excised and its capsular membranes were removed. The cells were dispersed by gentle stirring in ice-cold Hank's-HEPES buffer containing 0.1% BSA. The dispersed cells were filtered through cotton mesh sieves, followed by centrifugation at 50g for 1 min. The pellets containing parenchymal cells (PC) were washed twice with Hank's-HEPES buffer by centrifuging at 50g for 1 min. The supernatant containing NPC was similarly centrifuged twice. The resulting supernatant was then centrifuged twice at 200g for 2 min. PC and NPC were resuspended separately in ice-cold Hank's-HEPES buffer (4 mL for PC and 1.8 mL for NPC). The cell numbers and viability were determined by the trypan blue exclusion method. Then, the radioactivity in the cells (0.5 mL) was determined as for the other tissue samples.

### Statistical Analysis

Statistical comparisons were performed using Student's unpaired *t*-test. *p* < 0.05 was considered to be indicative of statistical significance.

## RESULTS

### Physicochemical Properties of Liposomes

The mean diameters of prepared liposomes were about 80–90 nm, respectively (Tab. 1). The particle sizes of the liposomes were kept constant for a period of at least 2 months at 4°C (data not shown).

### Lectin-Induced Aggregation of Liposomes

The exposure of galactose on the surface of liposomes was confirmed by measurement of amount of aggregation of liposomes caused by the lectin form *Ricinus communis* (RCA120). The aggregation was monitored at room temperature by the time-dependent increase in turbidity as measured by the absorbance at 350 nm. As shown in Figure 1, there was no lectin-mediated aggregation of bare-liposomes. In contrast, when the liposomes were modified with Gal-C4-Chol, slight lectin-induced aggregation was observed at a mole% of 1.0 and 2.5. A marked aggregation was observed at a mole% above 2.5, that were 3.5, 5.0 and 7.5. At 7.5 mole% of Gal-C4-Chol, complete aggregation was observed. Furthermore the addition of galactose to the suspension of Gal-liposomes-RCA120 aggregates induced a rapid reduction of turbidity. These results suggest that galactose residues were exposed on the liposomes and the aggregation depended on the amount of galactose residue on the liposomes.

**Table 1.** Lipid Composition and Mean Diameter of Liposomes

Formulations	Lipid Composition (Molar Ratio)	Mean Diameter (nm) <sup>a</sup>
Bare-liposomes	DSPC/Chol (60:40)	89.1 ± 6.4
Gal 1.0-liposomes	DSPC/Chol/Gal-C4-Chol (60:39:1.0)	84.3 ± 5.0
Gal 2.5-liposomes	DSPC/Chol/Gal-C4-Chol (60:37.5:2.5)	87.7 ± 2.4
Gal 3.5-liposomes	DSPC/Chol/Gal-C4-Chol (60:36.5:3.5)	86.8 ± 3.0
Gal 5.0-liposomes	DSPC/Chol/Gal-C4-Chol (60:35:5.0)	87.9 ± 3.0
Gal 7.5-liposomes	DSPC/Chol/Gal-C4-Chol (60:32.5:7.5)	78.5 ± 3.6

Each value represents the mean ± SD of three experiments.

<sup>a</sup>The mean diameter of liposomes was measured using a dynamic light-scattering spectrophotometer.

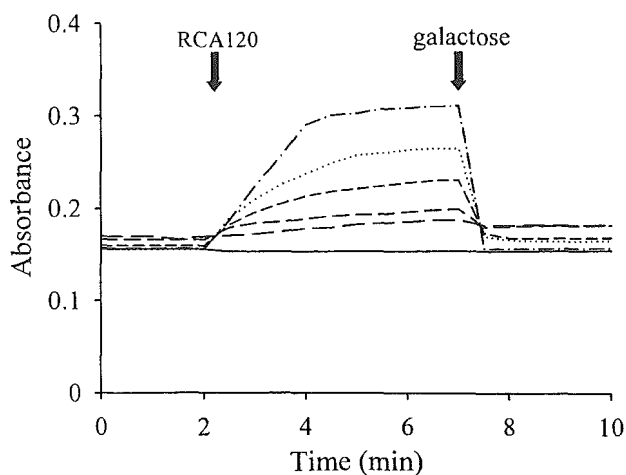


**Figure 1.** Time course of the turbidity change of bare: (—), Gal 1.0: (---), Gal 2.5: (- - -), Gal 3.5: (· · · ·), Gal 5.0: (— · — ·), and Gal 7.5: (— · — ·) liposomes after addition of RCA120 at 25°C. Liposomes (total lipid conc. 0.1 mg/mL) were added into a cuvette. One hundred microliters of RCA120 (1.0 mg/mL) was added to a cuvette at the appropriate time. After rapid mixing, aggregation of the liposomes was estimated by the time-dependent increase in turbidity as measure by the absorbance at 350 nm in a UV-3100 spectrometer. The reversibility of the aggregation was assessed by the addition of 100  $\mu$ L (10 mg/mL) free galactose.

### *In Vitro* Uptake of [ $^3$ H]CHE-Labeled Liposomes by HepG2 Cells

Figure 2 shows the *in vitro* uptake of [ $^3$ H]CHE-labeled liposomes by HepG2 cells. Gal-liposomes

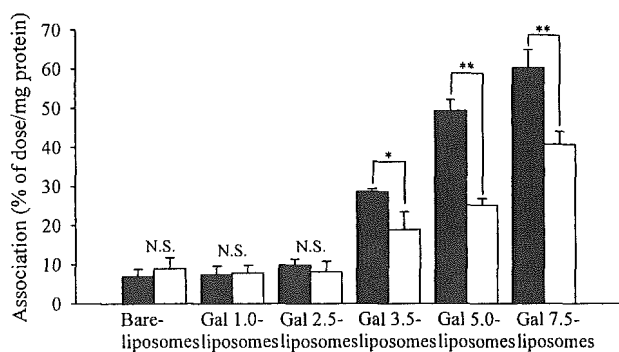


**Figure 2.** Uptake of [ $^3$ H]-labeled liposomes by HepG2 cells. Cells were incubated with each type of [ $^3$ H]-labeled liposomes with ( $\square$ ) or without ( $\blacksquare$ ) 20 mM galactose. The amount of [ $^3$ H]-radioactivity associated with the cells was measured following a 1 h incubation. Each value represents the mean  $\pm$  SD of three experiments. Statistically significant differences (\*:  $p < 0.05$ , \*\*:  $p < 0.01$ ) from liposomes incubated without 20 mM galactose. N.S., not significant.

having 1.0 and 2.5 mole% of Gal-C4-Chol were taken up by HepG2 cells to an extent that was comparable with that of bare-liposomes. On the other hand, the uptake of Gal-liposomes having 3.5, 5.0, and 7.5 mole% of Gal-C4-Chol, was much higher than that of bare-liposomes. In the presence of 20 mM galactose, the uptake of Gal-liposomes having 3.5, 5.0, and 7.5 mole% of Gal-C4-Chol was significantly inhibited, suggesting uptake by the asialoglycoprotein receptors.

The amount of surface binding and internalization of Gal-liposomes were evaluated using an acid-wash procedure. As shown in Figure 3, the surface binding of both bare-liposomes and Gal-liposomes having 1.0 and 2.5 mole% of Gal-C4-Chol was similar. Very little amounts of bare-liposomes and Gal-liposomes with 1.0 and 2.5 mole% of Gal-C4-Chol were internalized into the cells. In contrast, Gal-liposomes having 3.5, 5.0, and 7.5 mole% of Gal-C4-Chol showed a slight increase in surface binding and exhibited extensive uptake and internalization into HepG2 cells. These results suggest that the galactose density on the liposomal surface affects the ligand-receptor interaction that results in the different internalization of these Gal-liposomes into the cells.

### Biodistribution of [ $^3$ H]CHE-Labeled Liposomes

Figure 4 shows the blood concentration and liver accumulation-time course of [ $^3$ H]CHE-labeled bare and Gal-liposomes after intravenous injection into mice. Gal-liposomes having 3.5, 5.0, and 7.5 mole% of Gal-C4-Chol were rapidly eliminated from the blood circulation and mainly recovered in the liver, accounting for 80%, 86%, and 85% of the dose, respectively, within 10 min. As for Gal-liposomes having 1.0 and 2.5 mole% of Gal-C4-Chol, their liver accumulation slightly increased compared with bare-liposomes.

### Pharmacokinetic Analysis of Biodistribution of [ $^3$ H]CHE-Labeled Liposomes

To compare the disposition profiles of bare and Gal-liposomes, the initial distribution in the early phase up to 10 min, during which the contribution of metabolites can be ignored, was quantified using the tissue uptake clearance parameter. Table 2 summarizes the area under blood concentration-time curve (AUC) and tissue uptake clearances calculated for the initial 10 min for liver ( $CL_{\text{liver}}$ ), kidney ( $CL_{\text{kidney}}$ ), spleen ( $CL_{\text{spleen}}$ ), lung ( $CL_{\text{lung}}$ ), heart ( $CL_{\text{heart}}$ ), and urine ( $CL_{\text{urine}}$ )

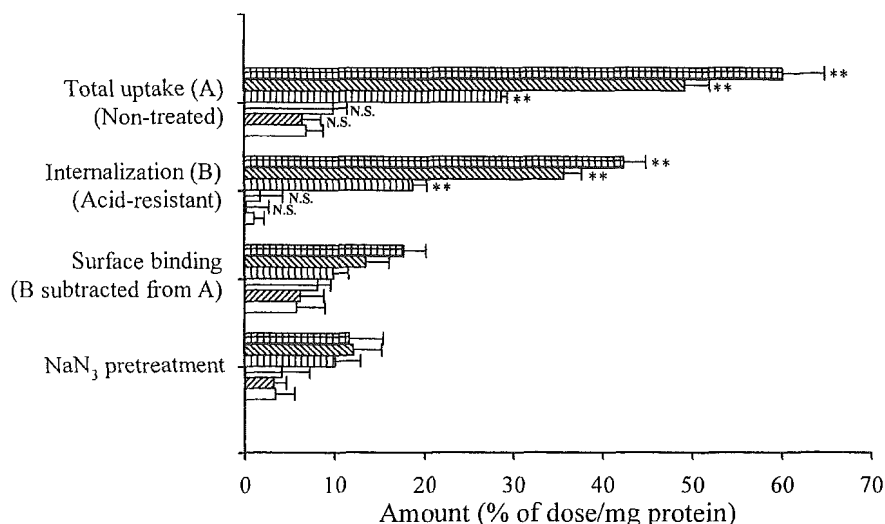


**Figure 3.** Amount of [ $^3\text{H}$ ]-labeled liposomes associated with HepG2 cells. Cells were incubated with bare ( $\square$ ), Gal 1.0 ( $\square$  with diagonal lines), Gal 2.5 ( $\square$  with horizontal lines), Gal 3.5 ( $\square$  with vertical lines), Gal 5.0 ( $\square$  with cross-hatch), or Gal 7.5 ( $\square$  with grid) liposomes. At 1 h after incubation, the cells were washed with an acid buffer to separate the surface bound liposomes. The difference in cellular association between acid-treatment and no treatment was regarded as the amount associated with the cell surface. In another group, the cells were preincubated with HBSS containing 10 mM  $\text{NaN}_3$  for 20 min prior to the addition of liposomes. Each value represents the mean + SD of three experiments. Statistically significant differences (\*\*:  $p < 0.01$ ) from bare-liposomes. N.S., not significant.

of [ $^3\text{H}$ ]CHE-labeled liposomes. The AUC of Gal-liposomes was lower than that of bare-liposomes. In particular, Gal-liposomes having 5.0 mole% of Gal-C4-Chol had the lowest AUC. The liver uptake clearance of Gal-liposomes having 1.0, 2.5, 3.5, 5.0, and 7.5 mole% of Gal-C4-Chol was 2.3, 4.2, 26, 67, and 60-times higher than that of bare-liposomes, respectively. Among the liposomes investigated, Gal-liposomes having 5.0

and 7.5 mole% of Gal-C4-Chol exhibited the highest liver uptake clearance.

#### Hepatic Cellular Localization of [ $^3\text{H}$ ]CHE-Labeled Liposomes

Figure 5 shows the hepatic cellular localization of [ $^3\text{H}$ ]CHE-labeled liposomes at 30 min after

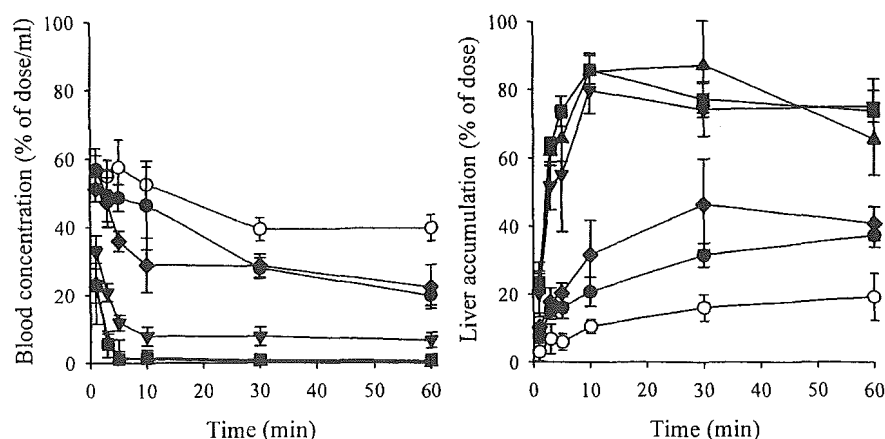


**Figure 4.** Time course of the concentration in blood and accumulation in liver of [ $^3\text{H}$ ]-labeled bare ( $\circ$ ), Gal 1.0 ( $\bullet$ ), Gal 2.5 ( $\blacklozenge$ ), Gal 3.5 ( $\blacktriangledown$ ), Gal 5.0 ( $\blacksquare$ ), and Gal 7.5 ( $\blacktriangle$ ) liposomes after intravenous injection in mice. Each value represents the mean  $\pm$  SD of three experiments.